



**HAL**  
open science

## Intumescent polypropylene in extreme fire conditions

Serge Bourbigot, Johan Sarazin, Tsilla Bensabath

► **To cite this version:**

Serge Bourbigot, Johan Sarazin, Tsilla Bensabath. Intumescent polypropylene in extreme fire conditions. *Fire Safety Journal*, 2020, 120, pp.103082. 10.1016/j.firesaf.2020.103082 . hal-02926318v2

**HAL Id: hal-02926318**

**<https://hal.univ-lille.fr/hal-02926318v2>**

Submitted on 28 May 2021

**HAL** is a multi-disciplinary open access archive for the deposit and dissemination of scientific research documents, whether they are published or not. The documents may come from teaching and research institutions in France or abroad, or from public or private research centers.

L'archive ouverte pluridisciplinaire **HAL**, est destinée au dépôt et à la diffusion de documents scientifiques de niveau recherche, publiés ou non, émanant des établissements d'enseignement et de recherche français ou étrangers, des laboratoires publics ou privés.

# 1 Intumescent polypropylene in extreme fire conditions

2 Serge Bourbigot<sup>a\*</sup>, Johan Sarazin<sup>a</sup>, Tsilla Bensabath<sup>a</sup>

3 <sup>a</sup>Univ. Lille, ENSCL, UMR 8207 - UMET - Unité Matériaux et  
4 Transformations, France, serge.bourbigot@ensc-lille.fr

5 \*Corresponding author

## 7 **Highlights:**

- 8 • Intumescent polypropylene (PP) can resist to burnthrough test
- 9 • Long time of piercing using zinc borate as synergist
- 10 • Borophosphates forming a glass reinforcing the intumescent char

## 12 **Abstract:**

13 The paper deals with intumescent polypropylene (PP) undergoing extreme  
14 fire (burn-through test with heat flux higher than 100 kW/m<sup>2</sup>). The purpose  
15 of this unusual approach is to explore the possibility to design intumescent  
16 plastic (here PP) resisting to burn-through test. A combination of  
17 commercial intumescent flame retardants (ammonium polyphosphate-based  
18 compounds containing a char former; AP766 (AP) and FlameOff (FO) of  
19 the companies Clariant and FlameOff Inc) with zinc borate (supplied by US  
20 Borax, ZB) or Kemgard (combination of ZB and molybdate supplied by  
21 Huber, KZ) was incorporated in PP. Use of ZB and KZ as synergists in FO  
22 formulations increases dramatically the time of piercing (formation of hole  
23 through the plaque of polymer at 80 s without ZB or KZ vs. 280 s with KZ)  
24 at the burn-through test (heat flux = 116 kW/m<sup>2</sup>, propane burner) while the  
25 combination with AP does not show any benefit. Analyses of the residues  
26 obtained at different times of combustion by solid state nuclear magnetic  
27 resonance (NMR) of <sup>31</sup>P, <sup>11</sup>B and <sup>13</sup>C shows the formation of  
28 borophosphates creating a glass reinforcing the intumescent char: it acts as  
29 a 'glue' providing flexibility and cohesion to the char.

31 **Keywords:** intumescence, fire chemistry, burn-through, polypropylene

## 33 **1. Introduction**

34 There is not a commonly accepted definition of the concept of 'extreme fire'.  
35 According to its common use the expression 'extreme fire' is a complex

36 entity as it involves different realities and ways of looking. It contains at  
37 least three concepts [1]: (i) an idea of extension in the sense that ‘extreme  
38 fire behavior’ is very commonly associated to very large fires or fires that  
39 extend in large areas during extended periods of time; (ii) an idea of intensity  
40 in the sense that some properties of fire spread, namely its rate of spread or  
41 its rate of energy release acquire very large values; (iii) a third idea that is  
42 associated to ‘extreme fire behavior’ is related to rapid change in fire  
43 behavior conditions that is also linked to some degree of uncertainty in its  
44 prediction and danger. In this paper, we only kept the idea of high rate of  
45 energy.

46 It is common practice by fire scientists to quantify the intensity of a fire by  
47 the radiant heat flux rather than flame temperature [2]. There is an  
48 approximate relationship between fire type and heat flux but we should  
49 recognize it is a crude assumption because the incident heat fluxes depend  
50 on the spatial arrangement between the flame and the receiving target. The  
51 examples give a direct measurement of the heat flux from the source and  
52 they are: (i) small smoldering fire: 2-10 kW/m<sup>2</sup>; (ii) trash can fire: 10-50  
53 kW/m<sup>2</sup>; (iii) room fire, open pool fire: 50-100 kW/m<sup>2</sup>; (iv) post-flashover  
54 room fire, confined pool fire: >100 kW/m<sup>2</sup>, (v) jet fuel fire, open jetfire: 100-  
55 200 kW/m<sup>2</sup> and (vi) confined jetfire, BLEVE: >200 kW/m<sup>2</sup>. In this research,  
56 heat flux corresponding to open jetfire or jet fuel fire was considered (it is  
57 high energy and hence it can be considered as extreme fire). Higher heat  
58 fluxes were not selected because the purpose was to investigate the response  
59 of an intumescent polypropylene (PP) in unconventional conditions for fire  
60 testing.

61 The intumescence process results from a combination of charring and  
62 foaming at the surface of the substrate [3]. The result of this process is the  
63 formation of a multicellular (alveolar) barrier, thick and non-flammable,  
64 which protects the substrate or residual material from heat or flame action.  
65 The charred layer acts as a physical barrier which slows down heat and mass  
66 transfer between gas and condensed phase. The formation of an intumescent  
67 char is a complicated process involving several critical aspects: rheology  
68 (expansion phase, viscoelasticity of char), chemistry (charring) and  
69 thermophysics (limitation of heat and mass transfer) [4]. This concept of  
70 intumescence enables to make flame retarded (FR) polymeric materials  
71 (including PP-based materials) exhibiting high performance in the case of  
72 reaction to fire (contribution of the material to fire growth) [5]. FR PPs are  
73 not used in the case of resistance of fire (ability of materials to resist the  
74 passage of fire and/or gaseous products of combustion), i.e. fire scenarios  
75 corresponding to burn-through, jetfire or structural response to fire, because  
76 they are not designed for this: they soften upon heating and fire can spread

77 out. Nevertheless, intumescent coatings applied on steel or composite act as  
78 efficient fire barrier and we believe we should reach acceptable performance  
79 using intumescent thermoplastics in the case of resistance of fire. It is an  
80 unconventional testing for thermoplastics and no paper reports this type of  
81 approach. At this time, there is no specific application for this type of  
82 materials and the motivation of this paper is to explore the possibility to  
83 design intumescent plastic (here PP) resisting to burn-through test.

84 The paper is organized in three parts. The first part is devoted to the design  
85 of the intumescent formulation in PP considering potential synergists. Based  
86 on the results of the first part, the second part deals with the determination  
87 of mechanism of action using specific analyses by solid state nuclear  
88 magnetic resonance (NMR). Finally, the effect of the fillers content  
89 (loading) determined in the first part and incorporated in PP is examined in  
90 the third part.

## 92 **2. Experimental**

### 93 **2.1. Materials**

94 Commercial grade of PP was used in this work: PP (ISPLEN PP 089 Y1E)  
95 was supplied by Repsol (Madrid, Spain). PP 089 Y1E has a melt flow rate  
96 (MFR) for a load of 2.16 g at 230°C of 31 g/10 min. Modified ammonium  
97 polyphosphate (AP) is the commercial grade of Clariant (Knapsak,  
98 Germany) with the brand name Exolit AP766. It is an intrinsic intumescent  
99 system containing 24 wt% phosphorus and 15 wt% nitrogen acting in  
100 synergy. Another modified ammonium polyphosphate as a powder was used  
101 from the company FlameOff (Raleigh, NC – USA) and hereafter called FO  
102 (the composition is proprietary). Zinc borate (ZB) was added in combination  
103 with the intumescent additives as potential synergist. Its composition is  
104  $2\text{ZnO}\cdot 3\text{B}_2\text{O}_3$  and it was supplied by the company US Borax (Boron, CA -  
105 USA) under the brand name Firebrake. Kemgard 700Z is a complex mixture  
106 of zinc molybdate/zinc borate (the composition is proprietary) from the  
107 company Huber Engineered Materials (Atlanta, GA - USA): it was also used  
108 in combination with the intumescent additives as potential synergist and it  
109 is hereafter called KZ.

### 110 **2.2. Processing and formulations**

112 The strategy was to blend PP with FRs in a twin-screw extruder. The total  
113 loading of FRs in PP was between 30 and 50 wt% varying the ratio between  
114 the intumescent additives (AP or FO) and the synergists (ZB or KZ). The

115 formulations prepared in this work are gathered in Table 1. Note the loading  
 116 of ZB and KZ is low compared to AP and FO to get the highest  
 117 reinforcement of the intumescent char [6, 7].

118  
 119  
 120

Table 1. Formulations of the intumescent PPs

| <b>Formulation</b> | <b>PP (wt%)</b> | <b>AP (wt%)</b> | <b>FO (wt%)</b> | <b>ZB (wt%)</b> | <b>KZ (wt%)</b> |
|--------------------|-----------------|-----------------|-----------------|-----------------|-----------------|
| PP                 | 100             | 0               | 0               | 0               | 0               |
| PP(70)-AP          | 70              | 30              | 0               | 0               | 0               |
| PP(70)-AP/ZB(28:2) | 70              | 28              | 0               | 2               | 0               |
| PP(70)-FO          | 70              | 0               | 30              | 0               | 0               |
| PP(70)-FO/ZB(29:1) | 70              | 0               | 29              | 1               | 0               |
| PP(70)-FO/ZB(28:2) | 70              | 0               | 28              | 2               | 0               |
| PP(70)-FO/ZB(27:3) | 70              | 0               | 27              | 3               | 0               |
| PP(70)-FO/ZB(25:5) | 70              | 0               | 25              | 5               | 0               |
| PP(70)-FO/KZ(29:1) | 70              | 0               | 29              | 0               | 1               |
| PP(70)-FO/KZ(28:2) | 70              | 0               | 28              | 0               | 2               |
| PP(70)-FO/KZ(27:3) | 70              | 0               | 27              | 0               | 3               |
| PP(70)-FO/KZ(25:5) | 70              | 0               | 25              | 0               | 5               |
| PP(50)-FO/ZB(29:1) | 50              | 0               | 48.3            | 1.7             | 0               |
| PP(50)-FO/ZB(28:2) | 50              | 0               | 46.7            | 3.3             | 0               |
| PP(50)-FO/ZB(27:3) | 50              | 0               | 45              | 5               | 0               |
| PP(50)-FO/ZB(25:5) | 50              | 0               | 41.7            | 8.3             | 0               |
| PP(50)-FO/KZ(29:1) | 50              | 0               | 48.3            | 0               | 1.7             |
| PP(50)-FO/KZ(28:2) | 50              | 0               | 46.7            | 0               | 3.3             |
| PP(50)-FO/KZ(27:3) | 50              | 0               | 45              | 0               | 5               |
| PP(50)-FO/KZ(25:5) | 50              | 0               | 41.7            | 0               | 8.3             |

121

122 Compounding was performed using HAAKE Rheomix OS PTW 16 twin-  
123 screw extruder. The extruder is a co-rotating intermeshing twin screw with  
124 a barrel length of 400 mm and screw diameter of 16 mm ( $L/D = 25$ ) with 10  
125 zones. PP and FRs were incorporated using two gravimetric side feeders into  
126 the extruder. Polymer flow rate is fixed to extrude about 500 g/h with a  
127 screw speed of 300 rpm. The temperature profile of the extruder from feeder  
128 to die was set at 200/ 200/ 200/ 200/ 200/ 170/ 185/ 180/ 200/ 200°C.

129

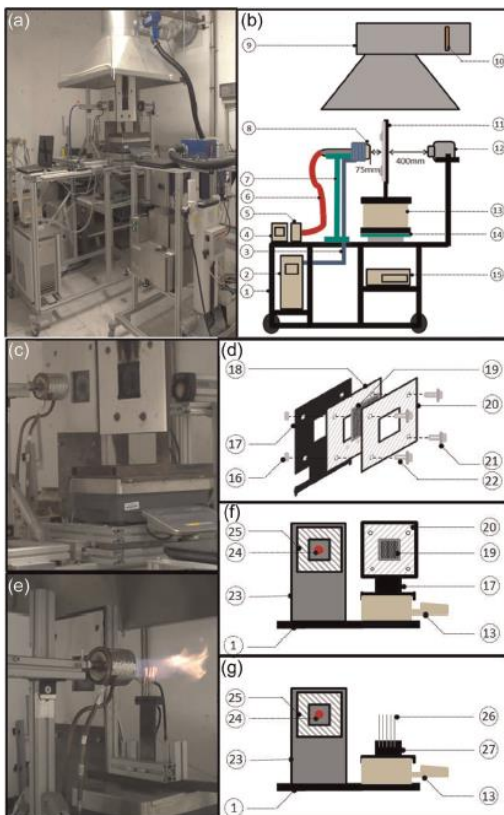
### 130 **2.3. Burn-through test**

131 In a previous work, a versatile fire test was developed with a complete set  
132 of instrumentation to investigate the fire behavior of materials. The  
133 description of this test is fully described in [8] and the reader could find all  
134 information about the setup and the measurement. In this paper, only  
135 required information to describe the operation of the test is given. This test  
136 is a burn-through test which was designed to mimic the aeronautical fire test  
137 defined in the standard ISO2685:1998. In this work, it was used as burn-  
138 through test and to create an extreme fire for fire-retarded thermoplastics.  
139 The equipment is described as follows and is shown in Fig. 1: (i) Propane  
140 burner from Bullfinch, (ii) High purity propane supplied by Air Liquide  
141 (N35, purity 99.95%), (iii) Propane flowmeter from Bronkhorst High-tech,  
142 (iv) Water-cooled heat flux gauge from Sequoia, (v) Cooling thermostat  
143 from Lauda Brinkmann (Lauda Proline RP845), (vi) Infrared (IR) camera  
144 from FLIR Systems™ (Thermovision™ A40M Researcher) calibrated  
145 from 0°C to 1000°C and (vii) Fireproof panels composed of silicate of  
146 calcium from Final Advanced Materials (Calsil) of 10mm thick.

147 The burner can deliver a propane-air flame characterized by a heat flux up  
148 to 200 kW/m<sup>2</sup>. The burner was placed at 75 mm from the material and the  
149 heat flux was calibrated at 116 kW/m<sup>2</sup> using a heat flux gauge in the same  
150 conditions as the tested sample in a separate box (error less than 5%). The  
151 temperature of the flame was measured with 5 aligned thermocouples (along  
152 the flame) at 1100°C. The sample size was 10x10 cm<sup>2</sup> and was put between  
153 the two panels in Calsil (see above). Temperature was measured in the center  
154 of the sample using a thermocouple embedded in the polymer at the surface  
155 of its backside. Infrared camera was also used to estimate the surface  
156 temperature assuming the emissivity of the surface constant equaling 0.92  
157 (black paint of known emissivity on the backside of the polymer plaque).  
158 Reasonable agreement was observed between the two measurements and  
159 only temperature measured by the thermocouple was shown in the  
160 following. All experiments were repeated at least twice and all

161 measurements were within 10% error (in [8], we showed the error on  
162 temperature measurement was less than 10%).

163



164

165

166

167

168

169

170

171

172

173

174

175

Fig. 1. Picture (a, c, e) and scheme (b, d, f, g) of the experimental apparatus - (1) Test bench frame, (2) Cooling system, (3) Copper coil cooler, (4) Propane thermocontroller, (5) Propane flowmeter, (6) Propane gas line, (7) Burner support, (8) Propane flame burner, (9) Hood, (10) Ring sampler, (11) Sample holder, (12) Infrared (IR) camera, (13) Precision scale, (14) Scale holder, (15) Data acquisition device, (16) Bolt, (17) Steel support, (18) Fireproof boards, (19) Sample, (20) Fireproof boards, (21) Washer, (22) Screw, (23) Water-cooled calorimeter holder, (24) Water-cooled calorimeter, (25) Fireproof panel, (26) Aligned thermocouples, (27) Thermocouple holder (adapted from [8])

176

## 2.4. NMR analyses

177

178

179

180

181

<sup>11</sup>B magic angle spinning – nuclear magnetic resonance (MAS-NMR) was performed at 256.6MHz on a 18.8 T Bruker Avance III spectrometer with a 3.2mm probehead operating at a spinning frequency ( $\nu_{rot}$ ) of 20 kHz. The spectra were recorded with a 1 ms pulse length (corresponding to a  $\pi/12$  flip angle determined on a liquid), a recycle delay (rd) of 10 s and 128 transients. <sup>13</sup>C and <sup>31</sup>P MAS-NMR experiments were performed on a 9.4 T Bruker

182 Avance spectrometer at 100.6 and 162MHz, respectively. The  $^{13}\text{C}(^1\text{H})$   
183 cross-polarization (CP) NMR experiment was conducted with a 4mm  
184 probehead at  $\nu_{\text{rot}}$  of 10 kHz with a 4 ms pulse length (corresponding to a  $\pi/2$   
185 flip angle), a rd of 10 s, a contact time of 1 ms and 1024 transients. The  $^{31}\text{P}$   
186 NMR analysis was carried out with a 4 mm probehead under  $^1\text{H}$  decoupling  
187 conditions. The spectrum was recorded with a  $\nu_{\text{rot}}$  of 12.5 kHz, a 2  $\mu\text{s}$  pulse  
188 length (corresponding to a  $\pi/4$  flip angle) a rd of 120 s and 16 transients.  $^{11}\text{B}$   
189 and  $^{31}\text{P}$  chemical shifts were referred to  $\text{NaBH}_4$  and  $\text{H}_3\text{PO}_4$  at - 42.06 ppm  
190 and 0 ppm, respectively.  
191

### 192 **3. Results and discussion**

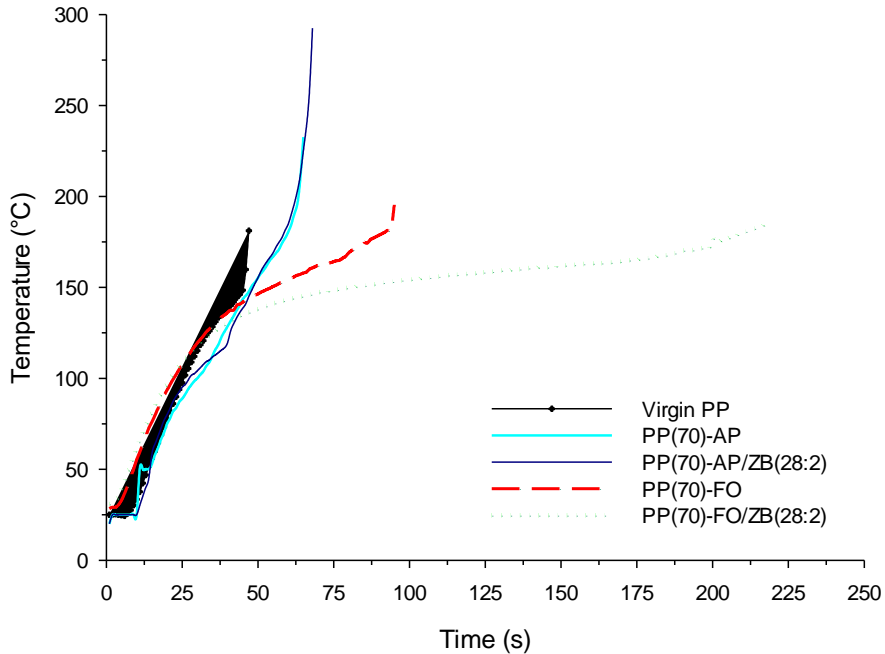
#### 193 **3.1. Design of the intumescent formulation**

194 Intumescent PPs are generally designed to exhibit high performance in terms  
195 of reaction to fire but not in terms of resistance to fire. In this section, it is  
196 our goal to examine the ability of intumescent PPs to resist to burn-through  
197 test. This condition is unusual for commodity polymer such as PP but  
198 intumescence is also used as protective coating for diverse substrates (e.g.  
199 steel, wood or composites) to pass the burn-through test. Two types of  
200 additives were incorporated in PP: (i) AP is a conventional intumescent  
201 additive providing low flammability to PP for various fire scenarios such as  
202 UL-94, glow wire or cone calorimeter and (ii) FO is a new intumescent  
203 additive on the market and was made from intumescent ingredients of  
204 intumescent paint. Based on previous works of this lab, zinc borate was  
205 selected as potential synergist because it is known to reinforce intumescent  
206 char [6]. ZB is a pure zinc borate and was already used in previous  
207 formulations [7] but KZ has never been evaluated in combination with  
208 intumescent ingredients. This last product was selected because its main  
209 composition is zinc borate and to take advantage of the presence of  
210 molybdate (known as synergist with metal hydroxides).

211 Intumescent PPs filled at 30 wt% loading were first evaluated (Fig. 2). The  
212 temperature rise in all materials is similar up to 40 s. Virgin PP softens when  
213 it reaches 140°C on its backside (melting temperature of PP is in the range  
214 150-170°C) and it pierces just after (sharp increase of temperature at 150°C).  
215 When AP and AP/ZB (ratio 28 to 2) are incorporated in PP, char formation  
216 at the surface of the material can be observed but it cannot extend the time  
217 to piercing. Visual observation suggests the expansion of the char is not fast  
218 enough to provide a protection and it remains too soft to resist to the  
219 impingement of the flame. In this case, there is no benefit to combine ZB  
220 with the intumescent additive. On the contrary, the incorporation of FO  
221 slows the temperature rise after 40 s thanks to the formation of an



222 intumescent char. The char resists to the impingement of the flame up to 90  
223 s and it pierces after because of the too high softening of the material. The  
224 addition of ZB in the formulation dramatically improves the resistance to  
225 piercing of the system. The time to piercing is reached at 225 s thanks to the  
226 fast formation of an intumescent char which remains rigid (low softening)  
227 for longer times.  
228



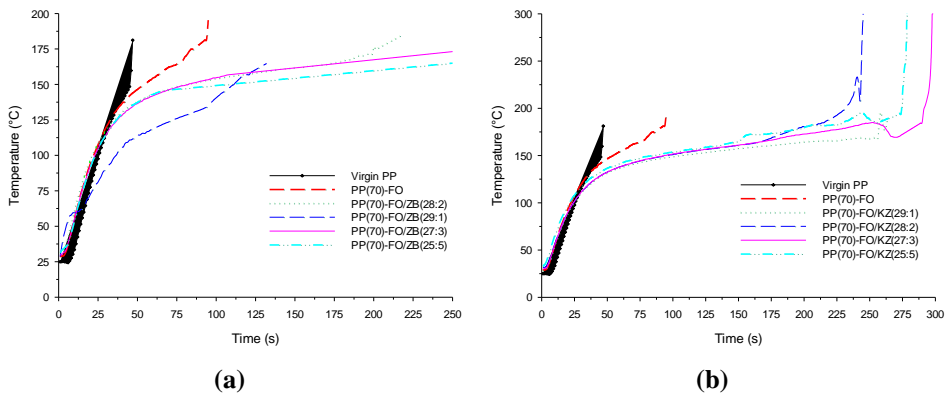
229  
230

231 Fig. 2. Temperature as a function of time on the backside of intumescent PPs containing  
232 AP and FO as main ingredient during a burn-through test at 116 kW/m<sup>2</sup>.

233 From the results above, it is shown AP is not the right additive for PP to  
234 perform the burn-through test. In the following, we only focus our work on  
235 FO in combination with ZB and on determining the best ratio FO/ZB. We  
236 kept the loading of ZB low compared to FO (Table 1) because our previous  
237 work showed the ratio intumescent formulation over ZB should be high  
238 enough (typically 28:2) to get the highest efficiency of ZB [7]. Fig. 3 –(a)  
239 shows the temperature/time curves of the formulations varying the ratio  
240 FO/ZB compared to virgin PP and PP(70)-FO. The formulation having the  
241 ratio 29:1 pierces at 125 s and so, it does not show any enhancement  
242 compared to the ratio 28:2. Note the performance is highly sensitive to the  
243 content of ZB: only 1wt% variation of ZB permits to gain 100s before  
244 piercing. The two ratios 27:3 and 25:5 enhance the time to piercing at 250 s  
245 compared to 225 s for the ratio 28:2. According to visual observation, the  
246 addition of ZB permits keeping the rigidity of the intumescent char

247 undergoing the impingement of the flame and preventing too much  
 248 deformation at longer times (and hence the piercing of the sample). The  
 249 same experiment was done substituting ZB by KZ with the same ratio (Fig.  
 250 3 –(b)). The addition of KZ in the formulations PP(70)-FO/KZ permits for  
 251 all ratios to dramatically enhance the time to piercing compared to the use  
 252 of FO alone. The behavior looks similar and the longer time to piercing is  
 253 reached at about 300 s for PP(70)-FO/KZ(25:5). The same conclusion as  
 254 above can be made namely the addition of KZ permits to reinforce the char  
 255 strength keeping its rigidity.

256



257 Fig. 3. Temperature as a function of time on the backside during a burn-through test at  
 258 116 kW/m² of (a) intumescent PP(70)-FO/ZB and (b) intumescent PP(70)-FO/KZ.

259

### 260 3.2. Role of zinc borate

261 The previous section showed the role of ZB reinforcing the intumescent  
 262 char. Specific chemical reactions should be responsible for this  
 263 reinforcement and were characterized by solid state NMR. This technique is  
 264 very useful because it permits the selection of the nucleus (here <sup>31</sup>P, <sup>11</sup>B and  
 265 <sup>13</sup>C) and to observe its surrounding. So, it gives the chemical species formed.  
 266 Four materials were selected based on the results above (best ratio of  
 267 FO/ZB=27/3): PP(70)-AP, PP(70)-AP/ZB(27:3), PP(70)-FO and PP(70)-  
 268 FO/ZB(27:3). Note ZB was used instead of KZ because the main component  
 269 of KZ is ZB and we wanted to avoid other additional interactions. They were  
 270 submitted at the burn-through test and the combustion was stopped at  
 271 characteristic times namely, 50 s (all samples), 100 s (samples containing  
 272 FO) and 215 s (only PP(70)-FO/ZB(27:3)). The samples before testing were  
 273 used as reference.

274 Ammonium polyphosphate (APP) is contained in both AP and FO and is  
275 one of the main ingredients of the intumescent flame retardants (Fig. 4 at  
276  $t=0$  s). Upon heating, APP decomposes and yields acidic phosphates acting  
277 as char promoter [3]. They play a significant role in the charring and in the  
278 formation of an intumescent coating: the evolution of the phosphate species  
279 should be revealed by  $^{31}\text{P}$  NMR. The four samples were then characterized  
280 by DD-MAS  $^{31}\text{P}$  NMR as a function of burning time (Fig. 4). The number  
281 of bridging oxygen atoms allows classifying the phosphate structure using  
282  $\text{Q}^n$  terminology where  $n$  represents the number of bridging oxygen atoms  
283 per phosphorus tetrahedron. This terminology was used in the following [9].  
284 The spectra of the neat materials ( $t = 0$  s) exhibit a doublet located at -22  
285 and -24 ppm assigned to  $\text{Q}^2$  site. This doublet is characteristic of P in APP  
286 as already reported in our previous work [10]. An additional band of low  
287 intensity at 1 ppm can be distinguished on the two FO samples. It is assigned  
288 to  $\text{Q}^0$  site probably an orthophosphate linked to aliphatic species.

289 At  $t = 50$  s, the two spectra of the samples without ZB exhibit three bands  
290 but not located at the same chemical shift (Fig. 4 (a) and (b)). The bands at  
291 0 and -12 ppm are common for the two materials and they are assigned to  
292  $\text{Q}^0$  site (probably mainly phosphoric acid [11]) and to  $\text{Q}^1$  site  
293 (orthophosphates linked to aromatic species [12]) respectively. It is  
294 noteworthy that the amount of species in  $\text{Q}^1$  site is higher than that in  $\text{Q}^0$  for  
295 PP(70)-FO (ratio of the areas  $\text{Q}^1/\text{Q}^0$  is higher). It suggests FO promotes the  
296 formation of phosphate linked to char. The band at -6 ppm (PP(70)-AP) is  
297 attributed to  $\text{Q}^2$  sites corresponding to pyrophosphates [12] and the broad  
298 band centered at -27 ppm (PP(70)-FO) is attributed to the formation of  
299 amorphous phosphate-type exhibiting  $\text{Q}^3$  and  $\text{Q}^4$  sites [13]. With the ZB in  
300 the formulation, the two systems have similar spectra (Fig. 4 (c) and (d)).  
301 The broad resonance (between 5 and -55 ppm) is the signature of a  
302 distributed structure found in glasses or amorphous compounds while the  
303 narrow resonances are characteristic of ordered phase. It can contain zinc  
304 phosphate and borophosphate in addition to phosphate glass [9, 10]. The two  
305 sharp bands at 0 and -6 ppm can be assigned as above. The band centered at  
306 -30 ppm is assigned to borophosphate [14] and the broad band centered at -  
307 12 ppm might be assigned as above in a disordered structure and/or to  
308 borophosphate glass [9]. Finally, at higher testing times for PP(70)-  
309 FO/ZB(27:3), the spectra are similar to those at 50s. Those results evidence  
310 APP and its decomposition products react with zinc borate. It is not unusual  
311 in intumescent systems and it was already reported in previous work [9].  
312 The formation of borophosphate glass reinforces the char and acts as a 'glue'  
313 providing flexibility and cohesion to the char.

314

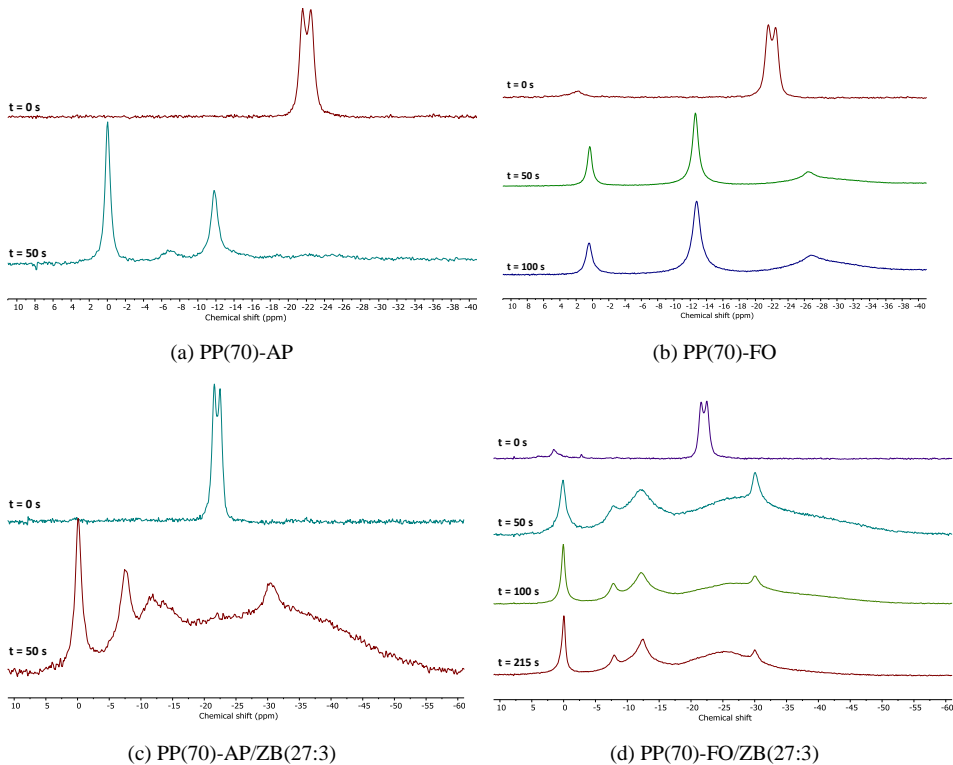


Fig. 4. DD-MAS  $^{31}\text{P}$  NMR of intumescent PPs as a function of burning time

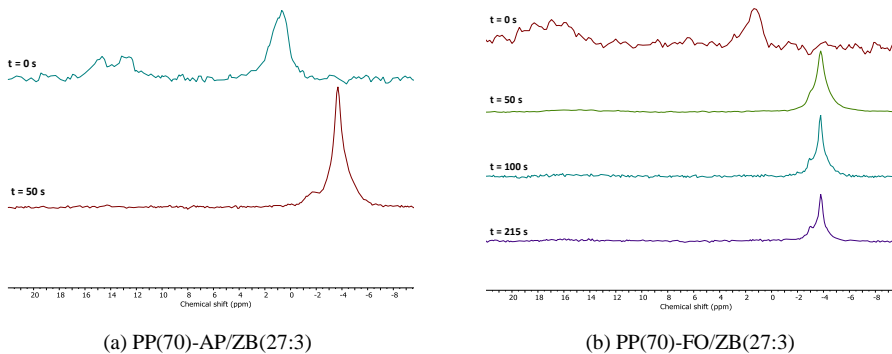
316

317

318 MAS  $^{11}\text{B}$  NMR spectra exhibit two bands at  $t=0\text{s}$  (Fig. 5). The first band  
 319 lying from 10 to 20 ppm, shows the presence of trigonal ( $\text{BO}_3$ ) borate units  
 320 while the second band (band centered around 1 ppm) is assigned to  
 321 tetragonal ( $\text{BO}_4$ ) borate species [9]. Those two polyhedra can be  
 322 characterized according to their different chemical shifts but also through  
 323 their quadrupolar constant ( $C_Q$ ).  $C_Q$  of  $\text{BO}_3$  is indeed much larger than that  
 324 of  $\text{BO}_4$  because of the higher asymmetry of the planar  $\text{BO}_3$  species (2.4-3.0  
 325 MHz and  $<1$  MHz for the  $\text{BO}_3$  and  $\text{BO}_4$  units, respectively) [15]. This  
 326 explains why  $\text{BO}_3$  signals are broader than  $\text{BO}_4$  resonances. After burning  
 327 ( $t > 0\text{s}$ ), the broad band assigned to  $\text{BO}_3$  units disappears and the band  
 328 assigned to  $\text{BO}_4$  units is shifted to -4 ppm (Fig. 5). The spectra are similar  
 329 for the two formulations and whenever the duration of testing. A main sharp  
 330 band can be distinguished at -4 ppm and a shoulder at -1.5 ppm which are  
 331 assigned to two types of borophosphates [16]. It is consistent with the  
 332 assignments of the DD-MAS  $^{31}\text{P}$  NMR spectra. Borates react with

333 phosphates upon heating and they are all consumed by the reaction: they are  
334 no longer 'free' borates in the intumescent coating.

335

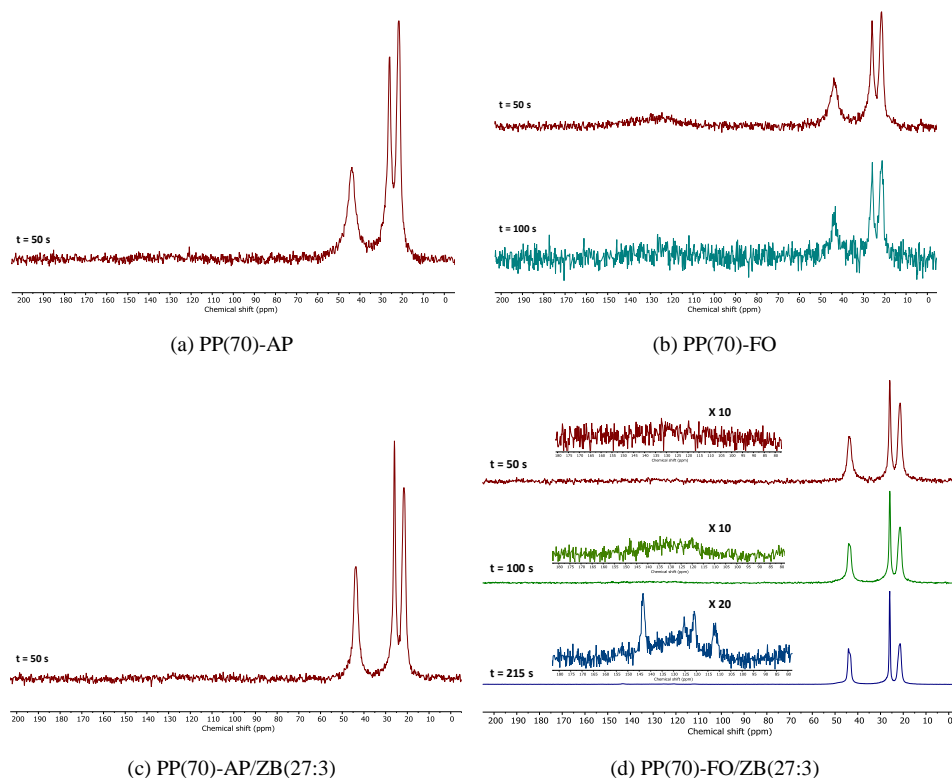


336 Fig. 5. MAS  $^{11}\text{B}$  NMR of intumescent PPs containing ZB as a function of burning time

337 The basic principle of intumescence is to make a protective char. Visual  
338 observation of the behavior of the materials evidences the charring of the 4  
339 systems and hence,  $^{13}\text{C}$  NMR should provide information on carbonaceous  
340 species formed upon burning. All CP-DD-MAS  $^{13}\text{C}$  NMR spectra exhibit  
341 three resonance bands located at 21, 26 and 43 ppm (Fig. 6). They can be  
342 assigned to polymeric chains of PP where the bands at 21, 26 and 43 ppm  
343 are assigned to  $\text{CH}_3$ ,  $\text{CH}$  and  $\text{CH}_2$  groups respectively [17]. For the sake of  
344 brevity, the spectra at  $t = 0$  s were not shown because they only exhibit the  
345 three mentioned bands and no additional insight was provided. It is  
346 noteworthy the bands of PP are detected whenever the duration of testing. It  
347 makes sense because the test is stopped when piercing occurs due to the  
348 softening of PP. PP is therefore not completely decomposed and so, it can  
349 be detected by NMR.

350 Intumescent char is constituted by condensed polyaromatic species  
351 containing mainly carbon and sometimes heteroatoms like nitrogen and  
352 oxygen [18, 19]. They are then detected by solid state NMR of carbon by a  
353 broad band centered around 130 ppm corresponding to  $\text{sp}^2$  hybridized  
354 aromatic carbon atoms. Except for the samples containing FO, this band  
355 cannot be detected with our experimental conditions (even when zooming  
356 in) (Fig. 6). Two phenomena could explain this: (i) CP was used for the  
357 acquisition of the spectra and because of the low number of protons on  
358 aromatic rings, the magnetization transfer is low and hence, the intensity of  
359 the band is low or undetectable and (ii) the formation of carbon free radicals  
360 on aromatic ring creates a strong anisotropy of magnetic susceptibility and  
361 then the loss of NMR signal [12]. Charring occurs for each sample and when  
362 detectable, a broad band centered at 125 ppm can be distinguished. On the

363 spectra recorded on FO containing samples at 50 s (Fig. 6-b) and at 100 s  
 364 (Fig. 6-d), a tail to the higher ppm is observed. It suggests the formation of  
 365 oxidized carbons and of aromatic carbons bound to phosphates [20].  
 366 Additional bands can be distinguished on the spectrum of PP(70)-  
 367 FO/ZB(27:3) at  $t = 215$  s (Fig. 6-d) located at 111, 121, 125 and 143 ppm.  
 368 They are relatively sharp on the broad band corresponding to the aromatic  
 369 carbons. The band at 111 ppm is assigned to protonated aromatic carbon,  
 370 those at 121 and 125 ppm are assigned to non-protonated aromatic carbons  
 371 and that at 143 ppm is assigned to aromatic carbons bound with phosphates  
 372 [20]. The shape of the 4 bands indicate carbon atoms are in an environment  
 373 of higher symmetry suggesting the formation of some crystalline species.  
 374 Overall, it is shown phosphates can be bound to the charred structure. The  
 375 presence of phosphate prevents the oxidation of ‘carbons’ [21] and provides  
 376 additional mechanical properties to the char (higher char strength and  
 377 flexibility) [22].



378 Fig. 6: CP-DD-MAS  $^{13}\text{C}$  NMR of intumescent PPs as a function of burning time

379  
 380

381

### 3.3. Effect of loading

382

383

384

385

386

387

388

389

390

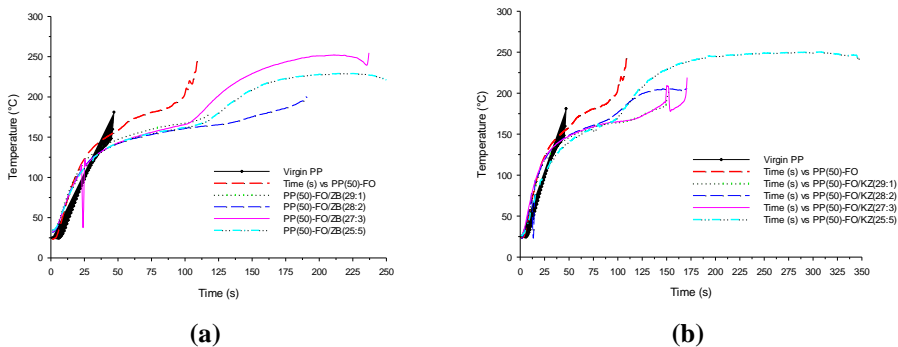
391

392

393

394

The first section showed that ZB and KZ in combination with FO provide superior performance at the burn-through test. The purpose is to increase the total loading of fillers (at 50 wt%) in PP to investigate its effect in terms of time to piercing. The time/temperature curves of all formulations are shown on Fig. 7. Surprisingly, the curves of the formulations containing ZB does not show any improvement compared to those at 30 wt% loading (Fig. 3 vs. Fig. 7). It is also true for the formulations containing KZ (times to piercing are even shorter) except for the ratio FO/KZ at 25 to 5 (Fig. 7-b). In this last case, the time to piercing reaches 330 s compared to the others exhibiting a time to piercing at 175 s. At high loading, it is observed higher charring but at the same time, the material looks softer. So, it implies that the impingement of the flame creates the piercing at shorter times because of its lower viscosity even if its efficiency as heat barrier might be higher.



395

396

397

Fig. 7. Temperature as a function of time on the backside during a burn-through test at 116 kW/m<sup>2</sup> of (a) intumescent PP(50)-FO/ZB and (b) intumescent PP(50)-FO/KZ.

398

### 4. Conclusion

399

400

401

402

403

404

405

406

407

408

409

410

This paper showed that intumescent PP could be designed to resist to burnthrough test. The selection of the intumescent system (or in another words the chemistry of the system) is essential to get long time to piercing (e.g. 100 s vs. 40 s when using FO instead of AP) and a synergist can dramatically extend the time to piercing (e.g. 215 s vs. 100 s when using FO/ZB instead of FO alone). Analyzing the residues obtained at different times of combustion by solid state NMR of <sup>31</sup>P, <sup>11</sup>B and <sup>13</sup>C, it is shown that phosphates were bound to the charred structure (in the case of FO containing systems) and that the formation of borophosphates created a glass reinforcing the intumescent char. This combination provides flexibility and cohesion to the char. The unusual fire resistance of FR plastics paves the way to other applications where burnthrough scenario can be involved. Such

411 scenario might happen in plants if leak of flammable products occurs  
412 creating a torch impinging surrounded plastics. The fire resistance of our  
413 formulations might bring therefore additional fire safety.  
414

## 415 **5. Acknowledgement**

416 This work has received funding from the European Research Council (ERC)  
417 under the European Union's H2020- the framework programme for  
418 Research and Innovation (2014-2020) ERC Grant Advances Agreement  
419 N°670747-ERC 2014 AdG/FireBar-Concept for FireBar Concept project.  
420

## 421 **6. References**

- 422 [1] Viegas DX. Extreme fire behaviour. In. Extreme fire behaviour. Nova Science  
423 Publishers, Inc., 2012, pp. 1-56.
- 424 [2] La Delfa G, Luinge JW, Gibson AG, Integrity of composite aircraft fuselage materials  
425 under crash fire conditions, *Plastics, Rubber and Composites*, 2009;38: 111-17.
- 426 [3] Alongi J, Han Z, Bourbigot S, Intumescence: Tradition versus novelty. A  
427 comprehensive review, *Progress in Polymer Science*, 2015;51: 28-73.
- 428 [4] Jimenez M, Duquesne S, Bourbigot S, Multiscale Experimental Approach for  
429 Developing High-Performance Intumescent Coatings, *Industrial & Engineering Chemistry*  
430 *Research*, 2006;45: 4500-08.
- 431 [5] Bourbigot S, Sarazin J, Bensabath T, Samyn F, Jimenez M, Intumescent  
432 polypropylene: Reaction to fire and mechanistic aspects, *Fire Safety Journal*, 2019;105:  
433 261-69.
- 434 [6] Casetta M, Delaval D, Traisnel M, Bourbigot S, Influence of the recycling process on  
435 the fire-retardant properties of PP/EPR blends, *Macromolecular Materials and*  
436 *Engineering*, 2011;296: 494-505.
- 437 [7] Fontaine G, Bourbigot S, Duquesne S, Neutralized flame retardant phosphorus agent:  
438 Facile synthesis, reaction to fire in PP and synergy with zinc borate, *Polymer Degradation*  
439 *and Stability*, 2008;93: 68-76.
- 440 [8] Tranchard P, Samyn F, Duquesne S, Thomas M, Estèbe B, Montès JL, Bourbigot S,  
441 Fire behaviour of carbon fibre epoxy composite for aircraft: Novel test bench and  
442 experimental study, *Journal of Fire Sciences*, 2015;33: 247-66.
- 443 [9] Hansupo N, Tricot G, Bellayer S, Roussel P, Samyn F, Duquesne S, Jimenez M,  
444 Hollman M, Catala P, Bourbigot S, Getting a better insight into the chemistry of  
445 decomposition of complex flame retarded formulation: New insights using solid state  
446 NMR, *Polymer Degradation and Stability*, 2018;153: 145-54.
- 447 [10] Samyn F, Bourbigot S, Duquesne S, Delobel R, Effect of zinc borate on the thermal  
448 degradation of ammonium polyphosphate, *Thermochimica Acta*, 2007;456: 134-44.
- 449 [11] Sut A, Greiser S, Jäger C, Schartel B, Synergy in flame-retarded epoxy resin:  
450 Identification of chemical interactions by solid-state NMR, *Journal of Thermal Analysis*  
451 *and Calorimetry*, 2017;128: 141-53.
- 452 [12] Bourbigot S, Le Bras M, Delobel R, Decressain R, Amoureux JP, Synergistic effect  
453 of zeolite in an intumescence process: Study of the carbonaceous structures using solid-  
454 state NMR, *Journal of the Chemical Society - Faraday Transactions*, 1996;92: 149-58.
- 455 [13] Mercier C, Montagne L, Sfihi H, Palavit G, Boivin JC, Legrand AP, Local structure  
456 of zinc ultraphosphate glasses containing large amount of hydroxyl groups: <sup>31</sup>P and <sup>1</sup>H



457 solid state nuclear magnetic resonance investigation, *Journal of Non-Crystalline Solids*,  
458 1998;224: 163-72.

459 [14] Jimenez M, Duquesne S, Bourbigot S, Intumescent fire protective coating: Toward a  
460 better understanding of their mechanism of action, *Thermochimica Acta*, 2006;449: 16-  
461 26.

462 [15] Hansen MR, Madsen GKH, Jakobsen HJ, Skibsted J, Refinement of borate structures  
463 from  $^{11}\text{B}$  MAS NMR spectroscopy and density functional theory calculations of  $^{11}\text{B}$   
464 electric field gradients, *Journal of Physical Chemistry A*, 2005;109: 1989-97.

465 [16] Tricot G, Ragueneau B, Silly G, Ribes M, Pradel A, Eckert H, P-O-B3 linkages in  
466 borophosphate glasses evidenced by high field  $^{11}\text{B}/^{31}\text{P}$  correlation NMR, *Chemical*  
467 *Communications*, 2015;51: 9284-86.

468 [17] Laupretre F, Bebelman S, Daoust D, Devaux J, Legras R, Costa JL, NMR,  
469 differential scanning calorimetry, and fourier transform infrared characterization of the  
470 crystalline degree and crystallite dimensions of ethylene runs in isotactic  
471 polypropylene/ethylene-propylene copolymer blends (iPP/EP), *Journal of Applied*  
472 *Polymer Science*, 1999;74: 3165-72.

473 [18] Bourbigot S, Le Bras M, Delobel R, Breant P, Tremillon J-M, Carbonization  
474 mechanisms resulting from intumescence - part II. Association with an ethylene  
475 terpolymer and the ammonium polyphosphate-pentaerythritol fire retardant system,  
476 *Carbon*, 1995;33: 283-94.

477 [19] Bourbigot S, Le Bras M, Delobel R, Gengembre L, XPS study of an intumescent  
478 coating II. Application to the ammonium polyphosphate/pentaerythritol/ethylenic  
479 terpolymer fire retardant system with and without synergistic agent, *Applied Surface*  
480 *Science*, 1997;120: 15-29.

481 [20] Karrasch A, Wawrzyn E, Scharrel B, Jäger C, Solid-state NMR on thermal and fire  
482 residues of bisphenol A polycarbonate/silicone acrylate rubber/bisphenol A bis(diphenyl-  
483 phosphate)/(PC/ SiR/BDP) and PC/SiR/BDP/zinc borate (PC/SiR/BDP/ZnB) - Part I: PC  
484 charring and the impact of BDP and ZnB, *Polymer Degradation and Stability*, 2010;95:  
485 2525-33.

486 [21] McKee DW, Spiro CL, Lamby EJ, The inhibition of graphite oxidation by  
487 phosphorus additives, *Carbon*, 1984;22: 285-90.

488 [22] Bourbigot S, Le Bras M, Delobel R, Trémillon JM, Synergistic effect of zeolite in an  
489 intumescence process: Study of the interactions between the polymer and the additives,  
490 *Journal of the Chemical Society - Faraday Transactions*, 1996;92: 3435-44.

491